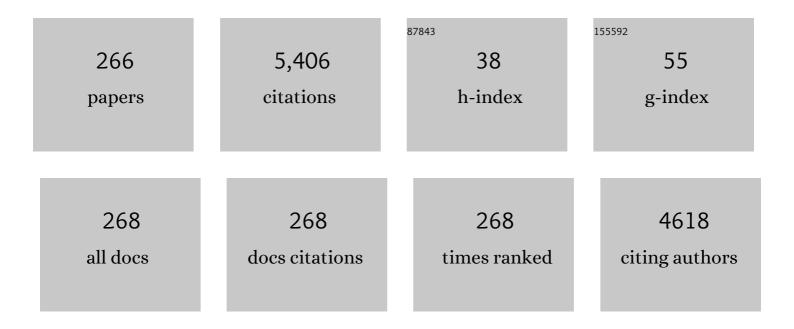
King-Chuen Lin

List of Publications by Year in descending order

Source: https://exaly.com/author-pdf/4757523/publications.pdf Version: 2024-02-01



#	Article	IF	CITATIONS
1	Unravelling the Multiple Emissive States in Citric-Acid-Derived Carbon Dots. Journal of Physical Chemistry C, 2016, 120, 1252-1261.	1.5	255
2	Recent Advances in Functionalized Carbon Dots toward the Design of Efficient Materials for Sensing and Catalysis Applications. Small, 2020, 16, e1905767.	5.2	217
3	Ultrathin Sulfur-Doped Graphitic Carbon Nitride Nanosheets As Metal-Free Catalyst for Electrochemical Sensing and Catalytic Removal of 4-Nitrophenol. ACS Sustainable Chemistry and Engineering, 2018, 6, 16021-16031.	3.2	137
4	Research Progress on Porous Carbon Supported Metal/Metal Oxide Nanomaterials for Supercapacitor Electrode Applications. Industrial & Engineering Chemistry Research, 2020, 59, 6347-6374.	1.8	132
5	Biomass-Derived Activated Carbon Supported Fe ₃ O ₄ Nanoparticles as Recyclable Catalysts for Reduction of Nitroarenes. ACS Sustainable Chemistry and Engineering, 2016, 4, 6772-6782.	3.2	108
6	Chemically Induced Fluorescence Switching of Carbon-Dots and Its Multiple Logic Gate Implementation. Scientific Reports, 2015, 5, 10012.	1.6	88
7	Biomass Derived Sheet-like Carbon/Palladium Nanocomposite: An Excellent Opportunity for Reduction of Toxic Hexavalent Chromium. ACS Sustainable Chemistry and Engineering, 2017, 5, 5302-5312.	3.2	79
8	Polymeric Ladderphanes. Journal of the American Chemical Society, 2009, 131, 12579-12585.	6.6	75
9	Detection of iron species using inductively coupled plasma mass spectrometry under cold plasma temperature conditions. Spectrochimica Acta, Part B: Atomic Spectroscopy, 2001, 56, 123-128.	1.5	70
10	Palladium and silver nanoparticles embedded on zinc oxide nanostars for photocatalytic degradation of pesticides and herbicides. Chemical Engineering Journal, 2021, 410, 128434.	6.6	63
11	Fabrication of Platinum–Rhenium Nanoparticle-Decorated Porous Carbons: Voltammetric Sensing of Furazolidone. ACS Sustainable Chemistry and Engineering, 2020, 8, 3591-3605.	3.2	57
12	Ultrathin 2D graphitic carbon nitride nanosheets decorated with silver nanoparticles for electrochemical sensing of quercetin. Journal of Electroanalytical Chemistry, 2018, 826, 207-216.	1.9	56
13	Pyrene-Based Chemosensor for Picric Acid—Fundamentals to Smartphone Device Design. Analytical Chemistry, 2019, 91, 13244-13250.	3.2	56
14	Highly stable ruthenium nanoparticles on 3D mesoporous carbon: an excellent opportunity for reduction reactions. Journal of Materials Chemistry A, 2015, 3, 23448-23457.	5.2	52
15	Characterization of Two Types of Silanol Groups on Fused-Silica Surfaces Using Evanescent-Wave Cavity Ring-Down Spectroscopy. Analytical Chemistry, 2007, 79, 3654-3661.	3.2	51
16	Well-dispersed rhenium nanoparticles on three-dimensional carbon nanostructures: Efficient catalysts for the reduction of aromatic nitro compounds. Journal of Colloid and Interface Science, 2017, 506, 271-282.	5.0	51
17	Highly sensitive fluorogenic sensing of L-Cysteine in live cells using gelatin-stabilized gold nanoparticles decorated graphene nanosheets. Sensors and Actuators B: Chemical, 2018, 259, 339-346.	4.0	50
18	Productions of I, I*, and C2H5 in the A-band photodissociation of ethyl iodide in the wavelength range from 245to283nm by using ion-imaging detection. Journal of Chemical Physics, 2007, 126, 064302.	1.2	48

#	Article	IF	CITATIONS
19	The correlation between ion production and emission intensity in the laser-induced breakdown spectroscopy of liquid droplets. Spectrochimica Acta, Part B: Atomic Spectroscopy, 2002, 57, 35-48.	1.5	47
20	Silicon Quantum Dot-Based Fluorescence Turn-On Metal Ion Sensors in Live Cells. ACS Applied Materials & amp; Interfaces, 2016, 8, 23953-23962.	4.0	47
21	Computational Studies of Versatile Heterogeneous Palladium-Catalyzed Suzuki, Heck, and Sonogashira Coupling Reactions. ACS Sustainable Chemistry and Engineering, 2017, 5, 8475-8490.	3.2	46
22	Alkali-hydrogen reactions. International Reviews in Physical Chemistry, 2002, 21, 357-383.	0.9	45
23	Molecular elimination of Br2 in 248 nm photolysis of bromoform probed by using cavity ring-down absorption spectroscopy. Journal of Chemical Physics, 2004, 121, 5253-5260.	1.2	45
24	Roads leading to roam. Role of triple fragmentation and of conical intersections in photochemical reactions: experiments and theory on methyl formate. Physical Chemistry Chemical Physics, 2014, 16, 2854-2865.	1.3	45
25	Determination of lanthanides in rock samples by inductively coupled plasma mass spectrometry using thorium as oxide and hydroxide correction standard. Spectrochimica Acta, Part B: Atomic Spectroscopy, 2003, 58, 809-822.	1.5	44
26	An overview of palladium supported on carbon-based materials: Synthesis, characterization, and its catalytic activity for reduction of hexavalent chromium. Chemosphere, 2020, 253, 126750.	4.2	44
27	MnCo ₂ O ₄ Microflowers Anchored on P-Doped <i>g</i> -C ₃ N ₄ Nanosheets as an Electrocatalyst for Voltammetric Determination of the Antibiotic Drug Sulfadiazine. ACS Applied Electronic Materials, 2021, 3, 3915-3926.	2.0	44
28	Stateâ€selective reaction of excited potassium atom with hydrogen molecule. K*+H2→KH+H. Journal of Chemical Physics, 1989, 90, 6151-6156.	1.2	43
29	Reaction pathway, energy barrier, and rotational state distribution for Li (2 2PJ)+H2→LiH (X 1Σ+)+H of Chemical Physics, 2001, 114, 9395-9401.	l. Journal 1.2	43
30	Aligned molecules: chirality discrimination in photodissociation and in molecular dynamics. Rendiconti Lincei, 2013, 24, 299-308.	1.0	43
31	Three-dimensional zinc oxide nanostars anchored on graphene oxide for voltammetric determination of methyl parathion. Mikrochimica Acta, 2020, 187, 17.	2.5	42
32	Development of Palladium on Bismuth Sulfide Nanorods as a Bifunctional Nanomaterial for Efficient Electrochemical Detection and Photoreduction of Hg(II) Ions. ACS Applied Materials & Interfaces, 2022, 14, 5908-5920.	4.0	42
33	Voltammetric determination of catechol and hydroquinone using nitrogen-doped multiwalled carbon nanotubes modified with nickel nanoparticles. Mikrochimica Acta, 2018, 185, 395.	2.5	41
34	Rotational population distribution of KH (v=0, 1, 2, and 3) in the reaction of K(5 2PJ, 6 2PJ, and 7 2PJ H2: Reaction mechanism and product energy disposal. Journal of Chemical Physics, 1996, 105, 9121-9129.	J) with 1.2	40
35	Photoinduced Electron Transfer in Silylene-Spaced Copolymers Having Alternating Donorâ^'Acceptor Chromophores. Macromolecules, 2007, 40, 2666-2671.	2.2	40
36	Temperature effect on nascent rotational state distribution of product MgH in reaction of Mg(3s3p1P1)+H2→MgH+H. Journal of Chemical Physics, 1989, 91, 5387-5391.	1.2	39

#	Article	IF	CITATIONS
37	Matrix effect on emission/current correlated analysis in laser-induced breakdown spectroscopy of liquid droplets. Spectrochimica Acta, Part B: Atomic Spectroscopy, 2004, 59, 321-326.	1.5	39
38	Two-step laser-assisted ionization of sodium in a hydrogen-oxygen-argon flame. Analytical Chemistry, 1981, 53, 1275-1279.	3.2	38
39	Mass-Analyzed Threshold Ionization Spectroscopy of 0-, m-, and p-Methylaniline Cations:  Vicinal Substitution Effects on Electronic Transition, Ionization, and Molecular Vibration. Journal of Physical Chemistry A, 2002, 106, 6462-6468.	1.1	38
40	Halogen Effect on the Photodissociation Mechanism for Gasâ€Phase Bromobenzene and Iodobenzene. ChemPhysChem, 2008, 9, 1130-1136.	1.0	38
41	Fluorescence turn-on chemosensors based on surface-functionalized MoS2 quantum dots. Sensors and Actuators B: Chemical, 2019, 281, 659-669.	4.0	38
42	Gold Nanoparticle Embedded on a Reduced Graphene Oxide/polypyrrole Nanocomposite: Voltammetric Sensing of Furazolidone and Flutamide. Langmuir, 2020, 36, 13949-13962.	1.6	38
43	Dynamical, spectroscopic and computational imaging of bond breaking in photodissociation: roaming and role of conical intersections. Faraday Discussions, 2015, 177, 77-98.	1.6	37
44	Multisensing Capability of MoSe ₂ Quantum Dots by Tuning Surface Functional Groups. ACS Applied Nano Materials, 2018, 1, 3453-3463.	2.4	37
45	Directions of chemical change: experimental characterization of the stereodynamics of photodissociation and reactive processes. Physical Chemistry Chemical Physics, 2014, 16, 9776.	1.3	36
46	Catalytic Activity of Bimetallic (Ruthenium/Palladium) Nanoâ€alloy Decorated Porous Carbons Toward Reduction of Toxic Compounds. Chemistry - an Asian Journal, 2019, 14, 2662-2675.	1.7	36
47	Collisional deactivation of K(7s 2S) and K(5d 2D) by H2. Journal of Chemical Physics, 1991, 94, 3529-3	536.2	35
48	Catalytic effect of a single water molecule on the OH + CH ₂ NH reaction. Physical Chemistry Chemical Physics, 2018, 20, 4297-4307.	1.3	35
49	Paper flower-derived porous carbons with high-capacitance by chemical and physical activation for sustainable applications. Arabian Journal of Chemistry, 2020, 13, 2995-3007.	2.3	35
50	Photodissociation of Propionaldehyde at 248 nm: Roaming Pathway as an Increasingly Important Role in Large Aliphatic Aldehydes. Journal of Physical Chemistry Letters, 2014, 5, 190-195.	2.1	34
51	Ultra-sensitive DNA sensing of a prostate-specific antigen based on 2D nanosheets in live cells. Nanoscale, 2017, 9, 12087-12095.	2.8	34
52	Activated porous carbon supported rhenium composites as electrode materials for electrocatalytic and supercapacitor applications. Electrochimica Acta, 2018, 271, 433-447.	2.6	34
53	Low-cost palladium decorated on <i>m</i> -aminophenol-formaldehyde-derived porous carbon spheres for the enhanced catalytic reduction of organic dyes. Inorganic Chemistry Frontiers, 2018, 5, 354-363.	3.0	34
54	Energy considerations in dual laser ionization processes in flames. Analytical Chemistry, 1983, 55, 2382-2387.	3.2	33

#	Article	IF	CITATIONS
55	Sr-Doped NiO ₃ nanorods synthesized by a simple sonochemical method as excellent materials for voltammetric determination of quercetin. New Journal of Chemistry, 2020, 44, 2821-2832.	1.4	33
56	Uncertainty propagation through correction methodology for the determination of rare earth elements by quadrupole based inductively coupled plasma mass spectrometry. Analytica Chimica Acta, 2005, 530, 91-103.	2.6	32
57	Ultrafine gold nanoparticle embedded poly(diallyldimethylammonium chloride)–graphene oxide hydrogels for voltammetric determination of an antimicrobial drug (metronidazole). Journal of Materials Chemistry C, 2020, 8, 7575-7590.	2.7	32
58	Species-Selected Mass-Analyzed Threshold Ionization Spectra of m-Fluoroaniline Cation. Applied Spectroscopy, 2001, 55, 120-124.	1.2	31
59	Influence of vibrational excitation on the reaction Li(2 2PJ)+H2(v=1)→LiH(X 1Σ+)+H. Journal of Chemical Physics, 2003, 119, 8785-8789.	1.2	31
60	Kinetic and Thermodynamic Investigation of Rhodamine B Adsorption at Solid/Solvent Interfaces by Use of Evanescent-Wave Cavity Ring-Down Spectroscopy. Analytical Chemistry, 2010, 82, 868-877.	3.2	31
61	Orientation dependence for Br formation in the reaction of oriented OH radical with HBr molecule. Physical Chemistry Chemical Physics, 2011, 13, 1419-1423.	1.3	31
62	Molecular elimination of methyl formate in photolysis at 234 nm: roaming vs. transition state-type mechanism. Physical Chemistry Chemical Physics, 2011, 13, 7154.	1.3	31
63	Functionalized Mesoporous Carbon Nanostructures for Efficient Removal of Eriochrome Black-T from Aqueous Solution. Journal of Chemical & Engineering Data, 2019, 64, 1305-1321.	1.0	31
64	State-specific reaction and product energy disposal of electronically excited potassium with hydrogen molecule. Journal of Chemical Physics, 1997, 107, 4244-4252.	1.2	30
65	Orientation dependence in the four-atom reaction of OH + HBr using the single-state oriented OH radical beam. Physical Chemistry Chemical Physics, 2010, 12, 2532.	1.3	30
66	Simple Preparation of Porous Carbon-Supported Ruthenium: Propitious Catalytic Activity in the Reduction of Ferrocyanate(III) and a Cationic Dye. ACS Omega, 2018, 3, 12609-12621.	1.6	30
67	Voltammetric determination of vitamin B2 by using a highly porous carbon electrode modified with palladium-copper nanoparticles. Mikrochimica Acta, 2019, 186, 299.	2.5	30
68	Laser-induced breakdown spectroscopy in analysis of Al3+ liquid droplets: On-line preconcentration by use of flow-injection manifold. Analytica Chimica Acta, 2007, 581, 303-308.	2.6	29
69	Communication: Photodissociation of CH3CHO at 308 nm: Observation of H-roaming, CH3-roaming, and transition state pathways together along the ground state surface. Journal of Chemical Physics, 2015, 142, 041101.	1.2	29
70	Roaming as the dominant mechanism for molecular products in the photodissociation of large aliphatic aldehydes. Physical Chemistry Chemical Physics, 2015, 17, 23112-23120.	1.3	29
71	A Metal-Free Carbon-Based Catalyst: An Overview and Directions for Future Research. Journal of Carbon Research, 2018, 4, 54.	1.4	29
72	Electrochemical sensor-based barium zirconate on sulphur-doped graphitic carbon nitride for the simultaneous determination of nitrofurantoin (antibacterial agent) and nilutamide (anticancer drug). Journal of Electroanalytical Chemistry, 2021, 901, 115782.	1.9	29

#	Article	IF	CITATIONS
73	Laser-induced breakdown spectroscopy of liquid droplets: correlation analysis with plasma-induced current versus continuum background. Journal of Analytical Atomic Spectrometry, 2005, 20, 53.	1.6	28
74	Laser-Enhanced Ionization Detection of Pb in Seawater by Flow Injection Analysis with On-Line Preconcentration and Separation. Analytical Chemistry, 1999, 71, 1561-1567.	3.2	27
75	Rotational energy transfer within CH A 2Δ(v=0) and B 2Σâ"(v=0) states by collisions with He, Ar, N2, CO, N2O, and CHBr3 using a time-resolved Fourier transform spectrometer. Journal of Chemical Physics, 2000, 112, 10204-10211.	1.2	27
76	248nm photolysis of CH2Br2 by using cavity ring-down absorption spectroscopy: Br2 molecular elimination at room temperature. Journal of Chemical Physics, 2006, 125, 133319.	1.2	27
77	Hexapole-Oriented Asymmetric-Top Molecules and Their Stereodirectional Photodissociation Dynamics. Journal of Physical Chemistry A, 2016, 120, 5389-5398.	1.1	27
78	Pyrene-based prospective biomaterial: In vitro bioimaging, protein binding studies and detection of bilirubin and Fe3+. Spectrochimica Acta - Part A: Molecular and Biomolecular Spectroscopy, 2019, 221, 117150.	2.0	25
79	Zinc and Sulfur Codoped Iron Oxide Nanocubes Anchored on Carbon Nanotubes for the Detection of Antitubercular Drug Isoniazid. ACS Applied Nano Materials, 2021, 4, 4562-4575.	2.4	25
80	Aptamer-based fluorogenic sensing of interferon-gamma probed with ReS2 and TiS2 nanosheets. Sensors and Actuators B: Chemical, 2018, 258, 929-936.	4.0	25
81	Collisional deactivation for K in high-lying2Sand2Dstates byH2. Physical Review A, 1992, 46, 3834-3839.	1.0	24
82	Br2 elimination in 248-nm photolysis of CF2Br2 probed by using cavity ring-down absorption spectroscopy. Journal of Chemical Physics, 2005, 123, 134312.	1.2	24
83	Photodissociation of CH3CHO at 248 nm by time-resolved Fourier-transform infrared emission spectroscopy: Verification of roaming and triple fragmentation. Journal of Chemical Physics, 2014, 140, 064313.	1.2	24
84	Graphene Oxide Nanosheets as An Efficient and Reusable Sorbents for Eosin Yellow Dye Removal from Aqueous Solutions. ChemistrySelect, 2017, 2, 3598-3607.	0.7	24
85	Highly Selective Voltammetric Sensor for <scp>l</scp> -Tryptophan Using Composite-Modified Electrode Composed of CuSn(OH) ₆ Microsphere Decorated on Reduced Graphene Oxide. Journal of Physical Chemistry C, 2020, 124, 25821-25834.	1.5	24
86	Vibrational and rotational population distributions of MgH(v''=0 and 1) produced in the reaction of Mg(3s3p1P1) withH2. Physical Review A, 1994, 50, 4891-4898.	1.0	23
87	Photodissociation of Gaseous Acetyl Chloride at 248 nm by Time-Resolved Fourier-Transform Infrared Spectroscopy: The HCl, CO, and CH ₂ Product Channels. Journal of Physical Chemistry A, 2010, 114, 7275-7283.	1.1	23
88	Photodissociation of dibromoethanes at 248 nm: An ignored channel of Br2 elimination. Journal of Chemical Physics, 2009, 130, 184308.	1.2	22
89	Rovibrationally Excited Molecules on the Verge of a Triple Breakdown: Molecular and Roaming Mechanisms in the Photodecomposition of Methyl Formate. Journal of Physical Chemistry A, 2016, 120, 5155-5162.	1.1	22
90	Photodissociation of CH ₃ CHO at 248 nm: identification of the channels of roaming, triple fragmentation and the transition state. Physical Chemistry Chemical Physics, 2017, 19, 18628-18634.	1.3	22

#	Article	IF	CITATIONS
91	Alignment effects in Ca–He(5 1P1–5 3PJ) energy transfer collisions by far wing laser scattering. Jourr of Chemical Physics, 1988, 89, 4771-4776.	1al 1.2	21
92	Ab initio calculation for potential energy surfaces relevant to the microscopic reaction pathways for Mg(3s3p1P1)+H2→MgH(2Σ+)+H. Journal of Chemical Physics, 1998, 108, 1475-1484.	1.2	21
93	Insight into the Photodissociation Dynamical Feature of Conventional Transition State and Roaming Pathways by an Impulsive Model. Journal of Physical Chemistry A, 2015, 119, 29-38.	1.1	21
94	Ultrafine Bi–Sn nanoparticles decorated on carbon aerogels for electrochemical simultaneous determination of dopamine (neurotransmitter) and clozapine (antipsychotic drug). Nanoscale, 2020, 12, 22217-22233.	2.8	21
95	Br2 molecular elimination in 248nm photolysis of CHBr2Cl by using cavity ring-down absorption spectroscopy. Journal of Chemical Physics, 2007, 126, 034311.	1.2	20
96	Photodissociation Dynamics of Bromofluorobenzenes Using Velocity Imaging Technique. Journal of Physical Chemistry A, 2008, 112, 1421-1429.	1.1	20
97	Stereodirectional images of molecules oriented by a variable-voltage hexapolar field: Fragmentation channels of 2-bromobutane electronically excited at two photolysis wavelengths. Journal of Chemical Physics, 2017, 147, 013917.	1.2	20
98	Quasiclassical Trajectory Calculations of Mg(3s3pP1) + H2 (ï = 0, N = 1) → MgH (ï, N) + H:  Trajectory and Angular Momentum Analysis on Improved ab Initio Potential Energy Surfaces. Journal of Physical Chemistry A, 2001, 105, 41-47.	1 1.1	19
99	Molecular Adsorption at Silica/CH3CN Interface Probed by Using Evanescent Wave Cavity Ring-Down Absorption Spectroscopy:Â Determination of Thermodynamic Properties. Analytical Chemistry, 2006, 78, 3583-3590.	3.2	19
100	Silver Nanoparticles Modified Graphitic Carbon Nitride Nanosheets as a Significant Bifunctional Material for Practical Applications. ChemistrySelect, 2017, 2, 1398-1408.	0.7	19
101	Binder-Free Modification of a Glassy Carbon Electrode by Using Porous Carbon for Voltammetric Determination of Nitro Isomers. ACS Omega, 2019, 4, 8907-8918.	1.6	19
102	Flame temperature determination by dual laser ionization. Chemical Physics Letters, 1982, 90, 111-116.	1.2	18
103	Collisional deactivation of potassium (52PJ) by molecular hydrogen. Identification of the primary quenching channel. The Journal of Physical Chemistry, 1984, 88, 6670-6675.	2.9	18
104	Reaction dynamics of Mg(3s3p 1P1) with CH4: Elucidation of reaction pathways for the MgH product by the measurement of temperature dependence and the calculation of ab initio potential energy surfaces. Journal of Chemical Physics, 1996, 104, 1370-1379.	1.2	18
105	Rotational and vibrational state distributions of NaH in the reactions of Na(4S2,3D2,and6S2) with H2: Insertion versus harpoon-type mechanisms. Journal of Chemical Physics, 2008, 128, 234309.	1.2	18
106	Recent Developments in Carbon-Based Nanocomposites for Fuel Cell Applications: A Review. Molecules, 2022, 27, 761.	1.7	18
107	I2 molecular elimination in single-photon dissociation of CH2I2 at 248 nm by using cavity ring-down absorption spectroscopy. Journal of Chemical Physics, 2011, 134, 034315.	1.2	17
108	AIE Nanodots Obtained from a Pyrene Schiff Base and Their Applications. ChemistrySelect, 2017, 2, 1353-1359.	0.7	17

#	Article	IF	CITATIONS
109	Photochemically Synthesized Ruthenium Nanoparticle-Decorated Carbon-Dot Nanochains: An Efficient Catalyst for Synergistic Redox Reactions. ACS Applied Materials & Interfaces, 2020, 12, 13759-13769.	4.0	17
110	Photodissociation dynamics of propionyl chloride in the ultraviolet region. Journal of Chemical Physics, 2009, 130, 014307.	1.2	16
111	Nonadiabatic Transition in the A-Band Photodissociation of Ethyl Iodide from 294 to 308 nm by Using Velocity Imaging Detection. Journal of Physical Chemistry A, 2009, 113, 35-39.	1.1	16
112	Gas-phase photodissociation of CH3COCN at 308 nm by time-resolved Fourier-transform infrared emission spectroscopy. Journal of Chemical Physics, 2012, 136, 044302.	1.2	16
113	Quasiclassical Trajectory Study of Mg(3s3pP1) + H2 Reaction on Fitted ab Initio Surfaces. Journal of Physical Chemistry A, 1999, 103, 7938-7948.	1.1	15
114	Temperature effect on the deactivation of electronically excited potassium by hydrogen molecule. Journal of Chemical Physics, 2000, 113, 4613-4619.	1.2	15
115	Photodissociation of gaseous CH3COSH at 248 nm by time-resolved Fourier-transform infrared emission spectroscopy: Observation of three dissociation channels. Journal of Chemical Physics, 2013, 138, 014302.	1.2	15
116	Mathematical Correction for Polyatomic Isobaric Spectral Interferences in Determination of Lanthanides by Inductively Coupled Plasma Mass Spectrometry. Journal of the Chinese Chemical Society, 2005, 52, 589-597.	0.8	14
117	Quasiclassical trajectory calculations for Li(22PJ) + H2 → LiH(X1Σ+) + H: Influence by vibrational excitation and translational energy. Journal of Chemical Physics, 2011, 134, 034119.	1.2	14
118	Regulation of nonadiabatic processes in the photolysis of some carbonyl compounds. Physical Chemistry Chemical Physics, 2016, 18, 6980-6995.	1.3	14
119	Roaming signature in photodissociation of carbonyl compounds. International Reviews in Physical Chemistry, 2018, 37, 217-258.	0.9	14
120	Roaming Dynamics and Conformational Memory in Photolysis of Formic Acid at 193 nm Using Time-resolved Fourier-transform Infrared Emission Spectroscopy. Scientific Reports, 2020, 10, 4769.	1.6	14
121	Polyol-assisted synthesis of spinel-type magnesium cobalt oxide nanochains for voltammetric determination of the antipsychotic drug thioridazine. Journal of Electroanalytical Chemistry, 2021, 898, 115600.	1.9	14
122	NMR Study of Some Sesquiterpene Alcohols and Their Oxidation Products. Journal of the Chinese Chemical Society, 1974, 21, 31-35.	0.8	13
123	Understanding product optimization: Kinetic versus thermodynamic control. Journal of Chemical Education, 1988, 65, 857.	1.1	13
124	Flow-Injection Inductively Coupled Plasma Mass Spectrometer Incorporated with an Ultrasonic Nebulizer-Membrane Dryer: Application to Trace Lead Detection in Aqueous Solution and Seawater. Applied Spectroscopy, 2001, 55, 604-610.	1.2	13
125	Fourier Transform Near-Infrared Absorption Spectroscopic Study of Catalytic Isomerization of Quadricyclane to Norbornadiene by Copper(II) and Tin(II) Salts. Journal of Physical Chemistry B, 2002, 106, 132-136.	1.2	13
126	Molecular halogen elimination from halogen-containing compounds in the atmosphere. Physical Chemistry Chemical Physics, 2014, 16, 7184.	1.3	13

#	Article	IF	CITATIONS
127	Application of Laser-Enhanced Ionization: Atomization Efficiency Determination. Applied Spectroscopy, 1992, 46, 1370-1375.	1.2	12
128	Rotational energy transfer of CH in the B (v=0) state by collisions with Ar and N2O using a time-resolved Fourier Transform spectrometer. Journal of Chemical Physics, 1997, 107, 10348-10349.	1.2	12
129	Br2 molecular elimination in photolysis of (COBr)2 at 248 nm by using cavity ring-down absorption spectroscopy: A photodissociation channel being ignored. Journal of Chemical Physics, 2011, 135, 234308.	1.2	12
130	Elimination mechanisms of Br2+ and Br+ in photodissociation of 1,1- and 1,2-dibromoethylenes using velocity imaging technique. Journal of Chemical Physics, 2011, 134, 194312.	1.2	12
131	Metal ion induced fluorescence resonance energy transfer between crown ether functionalized quantum dots and rhodamine B: selectivity of K+ ion. RSC Advances, 2015, 5, 4926-4933.	1.7	12
132	Carbon Dot Nanoparticles Exert Inhibitory Effects on Human Platelets and Reduce Mortality in Mice with Acute Pulmonary Thromboembolism. Nanomaterials, 2020, 10, 1254.	1.9	12
133	Application of Laser-Enhanced Ionization to Flame Temperature Determination. Applied Spectroscopy, 1991, 45, 1340-1343.	1.2	11
134	193 nm photodissociation of KI: Branching ratio and collisional mixing rate of K(5 2PJ) doublets. Journal of Chemical Physics, 1992, 96, 349-355.	1.2	11
135	Novel Technique To Reduce Electrical Interference Inherent in Laser-Enhanced Ionization Detection by Using Flow Injection Analysis. Analytical Chemistry, 1994, 66, 2180-2186.	3.2	11
136	Photodissociation of 1,2â€Dibromoethylene at 248 nm: Br ₂ Molecular Elimination Probed by Cavity Ringâ€Down Absorption Spectroscopy. ChemPhysChem, 2008, 9, 1137-1145.	1.0	11
137	Photodissociation of gaseous propionyl chloride at 248nm by time-resolved Fourier-transform infrared spectroscopy. Chemical Physics, 2010, 376, 1-9.	0.9	11
138	Interaction between crystal violet and anionic surfactants at silica/water interface using evanescent wave-cavity ring-down absorption spectroscopy. Journal of Colloid and Interface Science, 2012, 379, 41-47.	5.0	11
139	Vectorial imaging of the photodissociation of 2-bromobutane oriented <i>via</i> hexapolar state selection. Physical Chemistry Chemical Physics, 2019, 21, 14164-14172.	1.3	11
140	Laser-induced fluorescence of the B1Î-X1Σ+ band system of the isotopic lithium hydrides. Journal of Molecular Spectroscopy, 1988, 129, 388-394.	0.4	10
141	Spatially Resolved Temperature Determination of an Air/Acetylene Flame Using the Two-Step Laser-Enhanced Ionization Technique. Applied Spectroscopy, 1998, 52, 187-194.	1.2	10
142	The hetero Diels–Alder reactions of masked o-benzoquinones with nitroso compounds. Chemical Communications, 2001, , 1624-1625.	2.2	10
143	Dynamical and stereodynamical studies of alkaline-earth atom–molecule reactions. International Reviews in Physical Chemistry, 2007, 26, 289-352.	0.9	10
144	Gasâ€Phase Photodissociation of CH ₃ CHBrCOCl at 248 nm: Detection of Molecular Fragments by Timeâ€Resolved FTâ€IR Spectroscopy. ChemPhysChem, 2011, 12, 206-216.	1.0	10

#	Article	IF	CITATIONS
145	Metal Nanoparticles Anchored on Rhenium Disulfide Nanosheets as Catalysts for the Reduction of Aromatic Nitro Compounds. ChemNanoMat, 2018, 4, 1262-1269.	1.5	10
146	Internet of Things-Enabled Aggregation-Induced Emission Probe for Cu2+ lons: Comprehensive Investigations and Three-Dimensional Printed Portable Device Design. ACS Omega, 2020, 5, 32761-32768.	1.6	10
147	Effect of ammonia and water molecule on OH + CH3OH reaction under tropospheric condition. Scientific Reports, 2021, 11, 12185.	1.6	10
148	Determination of branching ratio and collisional mixing rate of potassium (52PJ) doublets following 193-nm photodissociation of potassium iodide in the presence of argon, helium, methane, and carbon dioxide. The Journal of Physical Chemistry, 1993, 97, 604-609.	2.9	9
149	Ion Enhancement Effect of Laser-Enhanced Ionization Induced by One-Step Excitation and Two-Step Excitation. Applied Spectroscopy, 1994, 48, 241-247.	1.2	9
150	Reaction dynamics of Mg(3 1P1, 4 1S0) with H2: insertion versus harpoon mechanism. Chemical Physics Letters, 1997, 274, 37-40.	1.2	9
151	Kinetics of Catalytic Isomerization of Quadricyclane to Norbornadiene Using Near Infrared Absorption Spectroscopy:Â Conversion Rate and Diffusion Motion in Heterogeneous Reaction. Journal of Physical Chemistry B, 2004, 108, 9364-9370.	1.2	9
152	Vibrational and rotational energy transfers involving the CH B Σâ^'2 v=1 vibrational level in collisions with Ar, CO, and N2O. Journal of Chemical Physics, 2006, 124, 144302.	1.2	9
153	Characterization of molecular channel in photodissociation of SOCl ₂ at 248 nm: Cl ₂ probing by cavity ring-down absorption spectroscopy. Physical Chemistry Chemical Physics, 2015, 17, 7838-7847.	1.3	9
154	Multifunctional Nanohybrid of Palladium Nanoparticles Encapsulated by Carbonâ€Dots for Exploiting Synergetic Applications. Advanced Materials Interfaces, 2019, 6, 1900361.	1.9	9
155	UV Photodissociation of Halothane in a Focused Molecular Beam: Space-Speed Slice Imaging of Competitive Bond Breaking into Spin–Orbit-Selected Chlorine and Bromine Atoms. Journal of Physical Chemistry A, 2020, 124, 5288-5296.	1.1	9
156	Ultrafine rhenium–ruthenium nanoparticles decorated on functionalized carbon nanotubes for the simultaneous determination of antibiotic (nitrofurantoin) and anti-testosterone (flutamide) drugs. Journal of Materials Chemistry C, 2021, 9, 15949-15966.	2.7	9
157	Alignment effects in Ca–He (5 1P1â^5 3PJ) energy transfer halfâ€collisions. Journal of Chemical Physic 1989, 90, 7605-7606.	^{cs,} 1.2	8
158	Ion Enhancement by Dual-Laser Ionization in an Acetylene/Air Flame. Applied Spectroscopy, 1989, 43, 20-24.	1.2	8
159	Experimental and Theoretical Study of Laser-Enhanced Ionization and Dual-Laser Ionization of Sodium Vapor. Applied Spectroscopy, 1989, 43, 66-74.	1.2	8
160	Photodissociation of (ICN)2 van der Waals dimer using velocity imaging technique. Journal of Chemical Physics, 2009, 130, 214305.	1.2	8
161	Probing the Ignored Elimination Channel of Br ₂ in the 248 nm Photodissociation of 1,1â€Đibromoethylene by Cavity Ringâ€Đown Absorption Spectroscopy. ChemPhysChem, 2009, 10, 672-679.	1.0	8
162	Photoinduced Electron Transfer of Oxazine 1/TiO2 Nanoparticles at Single Molecule Level by Using Confocal Fluorescence Microscopy. Langmuir, 2010, 26, 9050-9060.	1.6	8

#	Article	IF	CITATIONS
163	Reaction Dynamics with Molecular Beams and Oriented Molecular Beams: A Tool for Looking Closer to Chemical Reactions and Photodissociations. Journal of the Chinese Chemical Society, 2012, 59, 567-582.	0.8	8
164	Dynamics of chemical bond: general discussion. Faraday Discussions, 2015, 177, 121-154.	1.6	8
165	3D Probed Lipid Dynamics in Small Unilamellar Vesicles. Small, 2017, 13, 1603408.	5.2	8
166	Lightâ€Controlled Photochemical Synthesis of Gelatinâ€Capped Gold Nanoparticles for Spectral Activity and Electroâ€oxidation of Quercetin. ChemElectroChem, 2017, 4, 2842-2851.	1.7	8
167	Stereodynamic Imaging of Bromine Atomic Photofragments Eliminated from 1-Bromo-2-methylbutane Oriented via Hexapole State Selector. Journal of Physical Chemistry A, 2019, 123, 6635-6644.	1.1	8
168	Efficient and green synthesis of silver nanocomposite using guar gum for voltammetric determination of diphenylamine. Journal of Materials Science: Materials in Electronics, 2021, 32, 1289-1302.	1.1	8
169	Rydberg states and spin-orbit coupling of the thallium atom. Physical Review A, 1992, 46, 7150-7154.	1.0	7
170	Kinetic investigation of the quenching of Mg(3s3p 1P1) atoms in collisions with CH4 over the temperature range from 660 to 850 K. Journal of Chemical Physics, 1998, 109, 7821-7826.	1.2	7
171	Nascent rotational distribution and energy disposal of the CaH product in the reaction of Ca(4s4p 1P1)+H2→CaH(X 2â~+)+H. Journal of Chemical Physics, 1999, 111, 5277-5278.	1.2	7
172	Improvement in Data Acquisition for a Step-Scan Fourier Transform Spectrometer. Applied Spectroscopy, 1999, 53, 22-28.	1.2	7
173	Laser-enhanced ionization and laser-induced atomic fluorescence as element-specific detection methods for gas chromatography. Journal of Chromatography A, 2001, 921, 247-253.	1.8	7
174	A3Î1uâ†X1Σg+ laser photoacoustic spectroscopy of Br2 vapor in the extreme red wavelength region 665–720nm. Spectrochimica Acta - Part A: Molecular and Biomolecular Spectroscopy, 2004, 60, 1889-1893.	2.0	7
175	Multiple-Element Detection in Aqueous Solution and Seawater by Using an On-line Preconcentration Method for Inductively Coupled Plasma Mass Spectrometry. Analytical Sciences, 2006, 22, 1375-1378.	0.8	7
176	(1+1) Resonanceâ€Enhanced Multiphoton Ionization and Photodissociation Study of CS ₂ via the ¹ B ₂ State. ChemPhysChem, 2008, 9, 422-430.	1.0	7
177	Photodissociation of Dibromobenzenes at 266 nm by the Velocity Imaging Technique. ChemPhysChem, 2008, 9, 1721-1728.	1.0	7
178	Photodissociation of <i>cis</i> -, <i>trans</i> -, and 1,1-Dichloroethylene in the Ultraviolet Range: Characterization of Cl(² P _J) Elimination. Journal of Physical Chemistry A, 2010, 114, 37-44.	1.1	7
179	Competitive Bond Rupture in the Photodissociation of Bromoacetyl Chloride and 2―and 3â€Bromopropionyl Chloride: Adiabatic versus Diabatic Dissociation. ChemPhysChem, 2013, 14, 936-945.	1.0	7
180	Insight into photofragment vector correlation by a multi-center impulsive model. Physical Chemistry Chemical Physics, 2015, 17, 19592-19601.	1.3	7

#	Article	IF	CITATIONS
181	Roaming and chaotic behaviors in collisional and photo-initiated molecular-beam reactions: a role of classical vs. quantum nonadiabatic dynamics. Rendiconti Lincei, 2018, 29, 219-232.	1.0	7
182	<i>Ligusticum Striatum</i> -Derived Carbon Dots as Nanocarriers to Deliver Methotrexate for Effective Therapy of Cancer Cells. ACS Applied Bio Materials, 2020, 3, 8786-8794.	2.3	7
183	New observations on the B state of the CH radical from UV multiphoton dissociation of ketene. Chemical Physics Letters, 1995, 245, 585-590.	1.2	6
184	Automatic determination of optimum dilution levels for laser-enhanced ionization detection of matrix-interfered sample by flow injection. Analyst, The, 1995, 120, 2593.	1.7	6
185	lonization and dissociation mechanism of superexcited ketene using time-of-flight mass spectrometer. Journal of Chemical Physics, 1997, 107, 3797-3804.	1.2	6
186	Reaction dynamics of Mg(4 [sup 1]S[sub 0], 3 [sup 1]D[sub 2]) with H[sub 2]: Harpoon-type mech highly excited states. Journal of Chemical Physics, 2000, 113, 5302.	anism for 1.2	6
187	Spinâ€Resolved Rotational Energy Transfer for the CH B ² Σ ^{â^'} (<i>v</i> =0, N, F) State by Collisions with Ar. ChemPhysChem, 2008, 9, 572-578.	1.0	6
188	Alignment Selection of the Metastable CO(a ³ Î ₁) Molecule and the Steric Effect in the Aligned CO(a ³ Î ₁) + NO Collision. Journal of Physical Chemistry A, 2013, 117, 8157-8162.	1.1	6
189	Laserâ€induced Breakdown Spectroscopy of Liquid Droplets Based on Plasmaâ€induced Current Correlation. Journal of the Chinese Chemical Society, 2014, 61, 175-186.	0.8	6
190	DNA interaction probed by evanescent wave cavity ring-down absorption spectroscopy via functionalized gold nanoparticles. Analytica Chimica Acta, 2014, 820, 1-8.	2.6	6
191	Stereodirectional photodynamics: Experimental and theoretical perspectives. AIP Conference Proceedings, 2016, , .	0.3	6
192	Two-color resonant two-photon ionization and mass-analyzed threshold ionization spectroscopy of 4-chlorostyrene. Chemical Physics Letters, 2017, 682, 34-37.	1.2	6
193	Evanescent wave cavity ring-down spectroscopy based interfacial sensing of prostate-specific antigen. Sensors and Actuators B: Chemical, 2021, 330, 129284.	4.0	6
194	Effective Four-Center Model for the Photodissociation Dynamics of Methyl Formate. Lecture Notes in Computer Science, 2014, , 452-467.	1.0	6
195	Quantum yields of fragments in 193 nm photodissociation of KI. Chemical Physics Letters, 1992, 188, 37-41.	1.2	5
196	Collisional deactivation of K in the highâ€lying 2S and 2D states by He, Ne, and Ar. Journal of Chemical Physics, 1996, 105, 2719-2725.	1.2	5
197	Reaction pathway and energy disposal of the CaH product in the reaction of Ca(4s4p 1P1)+CH4→CaH(X 2â~+)+CH3. Journal of Chemical Physics, 2003, 118, 4938-4944.	1.2	5
198	Reaction pathway and potential barrier for the CaH product in the reaction of Ca(4s4p 1P1)+H2→CaH(X 2Σ+)+H. Journal of Chemical Physics, 2004, 120, 2774-2779.	1.2	5

#	Article	IF	CITATIONS
199	Molecular elimination of Br2 in photodissociation of CH2BrC(O)Br at 248 nm using cavity ring-down absorption spectroscopy. Journal of Chemical Physics, 2012, 137, 214304.	1.2	5
200	Interfacial Electron Transfer from CdSe/ZnS Quantum Dots to TiO ₂ Nanoparticles: Linker Dependence at Single Molecule Level. Electroanalysis, 2013, 25, 1064-1073.	1.5	5
201	Rotational state-selection and alignment of chiral molecules by electrostatic hexapoles. AIP Conference Proceedings, 2016, , .	0.3	5
202	Cl ₂ Elimination in 248 nm Photolysis of (COCl) ₂ Probed with Cavity Ring-Down Absorption Spectroscopy. Journal of Physical Chemistry A, 2017, 121, 2888-2895.	1.1	5
203	A Comparative Study of Chemicalâ€Initiated and Radiationâ€Induced Graft Copolymerization of Methyl Methacrylate onto Bamboo by Infrared Spectroscopic Technique. Journal of the Chinese Chemical Society, 1980, 27, 83-86.	0.8	4
204	Orbital alignment effect in a supersonic jet: spin-changing collisions in the Ca(4s5p 1P1)+Ar system. Chemical Physics Letters, 1992, 195, 579-585.	1.2	4
205	Reaction Dynamics of Mg(3s3p ¹ P ₁) with H ₂ . Journal of the Chinese Chemical Society, 1995, 42, 293-302.	0.8	4
206	lonization and dissociation mechanisms of ketene using resonance-enhanced multiphoton ionization mass spectrometer: (2+2) versus (2+1) schemes. Journal of Chemical Physics, 2001, 115, 7429-7435.	1.2	4
207	Two-Dimensional Correlation Analysis in Application to a Kinetic Model of Parallel Reactions. Applied Spectroscopy, 2003, 57, 168-175.	1.2	4
208	Interfacial Electron Transfer from CdSe/ZnS Quantum Dots to TiO ₂ Nanoparticles: Size Dependence at the Singleâ€Molecule Level. ChemPhysChem, 2012, 13, 2711-2720.	1.0	4
209	Stereodynamics: From elementary processes to macroscopic chemical reactions. AIP Conference Proceedings, 2015, , .	0.3	4
210	Photodissociation of CH ₂ BrI using cavity ring-down spectroscopy: in search of a BrI elimination channel. Physical Chemistry Chemical Physics, 2019, 21, 13943-13949.	1.3	4
211	Non-invasive and Time-dependent Blood-sugar Monitoring via Breath-derived CO2 Correlation Using Gas Chromatograph with a Milli-whistle Gas Analyzer. Analytical Sciences, 2020, 36, 739-743.	0.8	4
212	Architecting 3D prism shaped carbon dots/germanium/germanium oxide nanohybrid for photocatalytic degradation of pendimethalin and dinotefuran pesticides. Materials Today Chemistry, 2022, 24, 100913.	1.7	4
213	Laser Spectroscopy on the MgH A ² Π―X ² Σ ⁺ Band System. Journal of the Chinese Chemical Society, 1990, 37, 473-478.	0.8	3
214	The 248 nm photodissociation of KI: Determination of the branching ratio of K(4 2PJ) doublets in the presence of Ar, H2, and N2. Journal of Chemical Physics, 1993, 99, 9603-9607.	1.2	3
215	Applications of Laserâ€Enhanced Ionization In Analytical Chemistry. Journal of the Chinese Chemical Society, 1994, 41, 293-308.	0.8	3
216	Reaction dynamics of Mg(3s4s1S0) with H2: interference of the MgH product contribution from the lower Mg(3s3p1P1) state. Chemical Physics Letters, 1999, 304, 336-342.	1.2	3

#	Article	IF	CITATIONS
217	Two-Dimensional Correlation Analysis for a Kinetic Model of Consecutive Reactions. Applied Spectroscopy, 2003, 57, 1070-1077.	1.2	3
218	Reaction pathway for the nonadiabatic reaction of Ca(4s3dD1)+H2→CaH(XΣ+2)+H. Journal of Chemical Physics, 2005, 122, 084315.	1.2	3
219	Reaction dynamics of Ca(4s3dD21)+CH4→CaH(XΣ+2)+CH3: Reaction pathway and energy disposal for the CaH product. Journal of Chemical Physics, 2006, 124, 024304.	1.2	3
220	Catalytic Isomerization of Quadricyclane Using Fourier Transform Near-Infrared Absorption Spectroscopy:Â Diffusion, Conversion, and Temperature Effect. Journal of Physical Chemistry B, 2006, 110, 5563-5569.	1.2	3
221	Fine structure-resolved rotational energy transfer of SH (A ² Σ ⁺ , v′ = 0) state by collisions with Ar. Physical Chemistry Chemical Physics, 2010, 12, 1162-1171.	1.3	3
222	Note: Photodissociation of CH3COCN at 308 nm by time-resolved Fourier-transform infrared emission spectroscopy: Is CO a primary or secondary product?. Journal of Chemical Physics, 2013, 138, 246102.	1.2	3
223	Metal oxide-carbon nanocomposite-modified electrochemical sensors for toxic chemicals. , 2021, , 173-212.		3
224	Kinetic insights into ethynyl radical with isobutane and neopentane. Theoretical Chemistry Accounts, 2021, 140, 1.	0.5	3
225	Photodissociation study of spatially oriented (R)-3-bromocamphor by the hexapole state selector. Molecular Physics, 2022, 120, .	0.8	3
226	Emergent carbonized polymer dots as versatile featured nanomaterial for latent fingerprints, colorimetric sensor, and photocatalysis applications. Materials Today Nano, 2022, 20, 100246.	2.3	3
227	Application of Dual Laser Ionization to Trace Analysis of Sodium in A Flame. Journal of the Chinese Chemical Society, 1988, 35, 179-185.	0.8	2
228	Matrix Effect of Alkali and Alkaline Earth Metal Halides on Fluorescence Quantum Yield of Indium in Laserâ€Induced Fluorescence Flame Spectrometry. Journal of the Chinese Chemical Society, 2002, 49, 483-488.	0.8	2
229	Continuum and discrete pulsed cavity ring down laser absorption spectra of Br2 vapor. Spectrochimica Acta - Part A: Molecular and Biomolecular Spectroscopy, 2005, 61, 2115-2120.	2.0	2
230	Hydrogenâ€Bondingâ€Induced Oneâ€Handed Helical Polynorbornenes Appended With Chiral Alaninegland. Macromolecular Chemistry and Physics, 2011, 212, 2328-2338.	1.1	2
231	Decoherence Cross-Section in NO + Ar Collisions: Experimental Results and a Simple Model. Journal of Physical Chemistry A, 2013, 117, 8119-8125.	1.1	2
232	Coordinate Analysis for Interpreting the Decoherence in the Coherent NO with Ar Collision: A Physico-mathematical Picture Using the Stereographic Projection and the Cusp Catastrophe. Journal of the Chinese Chemical Society, 2017, 64, 25-35.	0.8	2
233	Cavity Ring-Down Absorption Spectroscopy: Optical Characterization of ICl Product in Photodissociation of CH ₂ ICl at 248 nm. Journal of Physical Chemistry A, 2018, 122, 8344-8353.	1.1	2
234	Temperature effect on water dynamics in tetramer phosphofructokinase matrix and the super-arrhenius respiration rate. Scientific Reports, 2021, 11, 383.	1.6	2

#	Article	IF	CITATIONS
235	Beyond the rule of transition state: Identification of roaming routes in some cases of carbonyl compounds. Journal of the Chinese Chemical Society, 2021, 68, 1358-1378.	0.8	2
236	Probing BrCl from photodissociation of CH ₂ BrCl and CHBr ₂ Cl at 248 nm using cavity ring-down spectroscopy. Physical Chemistry Chemical Physics, 2021, 23, 6098-6106.	1.3	2
237	A vector correlation study using a hexapole-oriented molecular beam: photodissociation dynamics of oriented isohaloethane. Physical Chemistry Chemical Physics, 2022, 24, 5914-5920.	1.3	2
238	Copper supported silica-based nanocatalysts for CuAAC and cross-coupling reactions. Reaction Chemistry and Engineering, 2022, 7, 1891-1920.	1.9	2
239	Comment on "Maximum Interaction Model of Force Constant Calculation of the ML _x (CO) _{6â€x} Type Molecule― Journal of the Chinese Chemical Society, 1976, 23, 75-80.	0.8	1
240	Near IR emission in sodium vapor under multiple excitations. AIP Conference Proceedings, 1988, , .	0.3	1
241	Observation of anti-Stokes-stimulated Raman scattering and two-photon emission in lithium and sodium vapors. AIP Conference Proceedings, 1988, , .	0.3	1
242	Dynamics and Kinetics of Metal Atoms in the Gas Phase. Journal of the Chinese Chemical Society, 1992, 39, 511-527.	0.8	1
243	Application of Laserâ€Enhanced Ionization Spectroscopy: Effect of Dissociation Constant on the Atomization Efficiency Determination in an Acetyleneâ€Air Flame. Journal of the Chinese Chemical Society, 2001, 48, 977-981.	0.8	1
244	Influence of vibrational excitation on the nonadiabatic reactions of metal atoms with H2. Journal of Chemical Physics, 2005, 123, 121101.	1.2	1
245	Doublet rotational energy transfer of the SH (X 2Î, v′′ = 0) state by collisions with Ar. Physical Chemistry Chemical Physics, 2011, 13, 8857.	1.3	1
246	Photodissociation of methyl formate: Conical intersections, roaming and triple fragmentation. AIP Conference Proceedings, 2015, , .	0.3	1
247	Role of cooperative network interaction in transition region of roaming reactions: Non-equilibrium steady state vs. thermal equilibrium reaction scheme. AIP Conference Proceedings, 2017, , .	0.3	1
248	Angular distribution of bromine atomic photofragment in oriented 2-bromobutane via hexapole state selector. AIP Conference Proceedings, 2017, , .	0.3	1
249	Halogen-related photodissociation in atmosphere: characterisation of atomic halogen, molecular halogen, and hydrogen halide. International Reviews in Physical Chemistry, 2021, 40, 1-50.	0.9	1
250	2D Fluorescence Correlation to Visualize Influence of Size Curvature and Phase Structure of Silica Nanoparticle-Supported Small Unilamellar Vesicle Membrane. Journal of Molecular Liquids, 2021, 344, 117949.	2.3	1
251	xmlns:mml="http://www.w3.org/1998/Math/MathML"> <mml:msub><mml:mi mathvariant="normal">Pb<mml:mn>6</mml:mn></mml:mi </mml:msub> <mml:msub><mml:mi mathvariant="normal">Co<mml:mn>9</mml:mn></mml:mi </mml:msub> <mml:mo>(</mml:mo> <mml:msub><</mml:msub>	111 mmi:mi) T	j E [†] Qq1_1 0.3
252	Study of cholesterol phase effect on the dynamics of DOPC and DPPC small vesicle membranes using single-molecule fluorescence correlation spectroscopy. Journal of Molecular Liquids, 2022, 353, 118806.	2.3	1

#	Article	IF	CITATIONS
253	Effect of High Order Coulombic Interaction on Radiationless Resonance Transfer of Electronic Excitation. Journal of the Chinese Chemical Society, 1976, 23, 127-137.	0.8	0
254	Alignment effects in Ca-He (51P1-53PJ) energy transfer half-collisions. AIP Conference Proceedings, 1989, , .	0.3	0
255	Collisional Deactivation of K(7s ² S) and K(5d ² D) by No. Journal of the Chinese Chemical Society, 1990, 37, 173-182.	0.8	0
256	<title>UV laser photolysis of KI: determination of quantum yield fine-structure branching ratio and collisional mixing rates of photofragments</title> . , 1993, 1858, 406.		0
257	Nascent Rotational Distributions of MgH in Reaction of Mg(4s ¹ S ₀) with H ₂ and HD. Journal of the Chinese Chemical Society, 1997, 44, 463-468.	0.8	0
258	Vibrationally selective radiative and non-radiative transitions in gaseous hydrogen molecules. Spectrochimica Acta - Part A: Molecular and Biomolecular Spectroscopy, 2011, 79, 396-399.	2.0	0
259	Quantum decoherence mechanism in atom-molecule - collisions: NO+Ar case study. , 2012, , .		0
260	Rotational Energy Transfer of SH(X ² Î, <i>v</i> â€2â€2=0, <i>J</i> â€2â€2=0.5–10.5) by Collision w Λâ€Doublet Resolved Transition Propensity. ChemPhysChem, 2012, 13, 274-280.	ith Ar: 1.0	0
261	Computational and Experimental Analysis of Carbon Functional Nanomaterials. , 2020, , 269-311.		0
262	Photodissociation of CH ₂ BrCHBrC(O)Cl at 248 nm: probing Br ₂ as the primary fragment using cavity ring-down spectroscopy. Physical Chemistry Chemical Physics, 2021, 23, 22492-22500.	1.3	0
263	Photo-Induced Electron Transfer from Dye or Quantum Dot to TiO2 Nanoparticles at Single Molecule Level. , 0, , .		0
264	Evanescent Wave Cavity Ring-down Spectroscopy in Application to Chemical and Biological Sensing. , 2014, , .		0
265	Graphitic carbon nitride for supercapacitor. , 2022, , 301-340.		0
266	Graphitic carbon nitride for photodegradation of dye Molecules. , 2022, , 97-140.		0